PORE WATER EFFECTS ON SOIL ERODIBILITY AND ITS IMPLICATION IN EPHEMERAL GULLY EROSION MODELING

Sayjro Nouwakpo, Purdue University, W. Lafayette, IN, snouwakp@purdue.edu and Chi-hua Huang, USDA-ARS, W. Lafayette, IN, chi-hua.huang@ars.usda.gov

Abstract Ephemeral gully erosion is the main source of sediment from the agricultural landscape, unfortunately, it has been overlooked in traditional soil erosion assessment. Field observations, and subsequent support from controlled lab experiments, have shown the linkage between transient soil hydraulic condition and initiation of rills or incised channels, specifically when the soil was oversaturated and exfiltration or upward seepage occurred. In order to properly account for this hydraulic effect, we propose to modify the soil erodibility parameters to accommodate the transient soil moisture condition. We used a mini-flume and empirically measured rill erodibility and critical shear stress of a silt loam soil under free drainage, saturation and upward seepage conditions. The mini-flume results showed similar magnitudes of soil loss as compared to a prior study performed on a 5m long 1.2 m wide soil box which required a large amount of soil just to fill the box. We then used two separate approaches to quantify the hydraulic condition when sediment detachment was initiated. The first technique was to use the mini flume and observe the incipient sediment detachment as flow shear stress was increased. The second approach was based on the fluidized bed principle to calculate the head loss at fluidization or incipient failure. By comparing the fluidization velocity of the cohesive soil to that of an equally dense non-cohesive material, we calculated the inherent soil cohesion. This result led to the calculation of critical shear stress at different vertical hydraulic gradients. We plan to incorporate this erodibility adjustment with soil profile and topographic attributes in a hillslope hydrologic model to quantify ephemeral gully development.

INTRODUCTION

Ephemeral gully is a transitional landscape feature which bears the characteristics of both hillslope and channel erosion processes. Quantification of ephemeral gully erosion has been challenging because it requires information on landscape attributes that are not normally considered in hillslope and channel erosion assessment models. For example, ephemeral gullies are often found in localized low spots or topographic convergence on hillslopes, therefore to properly model the gully occurrence would require a topographic model that are sufficiently detail to reflect these surface features. Although the ephemeral gully resembles an incised channel, the temporal and spatial variations of the location and geometry make it difficult to quantify and apply a well-defined channel hydraulics and erosion model. Figure 1 is an example of the ephemeral gully commonly found in the farm fields at the US Midwest.

Many scientists (Huang and Laflen, 1996; Bryan and Rockwell, 1998; Owoputi and Stolte, 2001; Römkens et al., 2001; Simon and Collison, 2001; Fox et al., 2006; Fox et al., 2007) have shown empirically that soil erosion varies depending on the vertical hydraulic gradient at the surface, or the pore water pressure. Using a 5m long, 1.2m wide and 0.3m deep soil box and laboratory rainfall simulation, Huang and Laflen (1996) and Zheng et al. (2000) showed that positive pore water pressure due to seepage increased sediment discharge when compared to the drainage condition, when the pore water was under tension, and the sediment load increased as the pore water pressure was increased from negative (drainage) to positive (seepage). Bryan and

Rockwell (1998) found a 20 to 30 fold increase of sediment transport rates after the water table was present at the surface. The impact of soil water pressure on soil detachment was also investigated by Römkens et al. (2001) who found that subsurface soil water pressure substantially affected sediment concentration in runoff but only marginally impacted the runoff amount. Owoputi and Stolte (2001) found increased soil loss when seepage was present in two study soils and attributed the increase to the changes in soil erodibility.

Figure 1 A typical ephemeral gully found in US Midwest farm fields.

In studying stream bank stability, Simon and Collison (2001) showed that forces during hydrograph recession may be large enough to substantially alter the erodibility of a cohesive streambed. Fox et al. (2007) found that the presence of seepage undercutting had a major effect on streambank stability.

Nachtergaele et al. (2001) studied gullies in the Belgian loess belt and identified different hydrologic conditions for gullies formed between summer and winter seasons with surface shear under intensive storms being the main driving factor for the summer gully and profile saturation or subsurface flow the cause for winter/spring gully development. Example of summer and winter gullies are shown in Figure 2. Comparing the photos from the field to those obtained from the controlled laboratory experiments (Figure 3), where the near-surface hydraulic gradient or pore water pressure at the surface was controlled, it became evident that the near-surface hydraulic gradient indeed affected how the surface was eroded and the pore water pressure controlled by the subsurface hydrology, i.e., drainage vs. seepage gradient, needs to be accounted for in assessing ephemeral gully erosion. From a geomorphic point of view, if ephemeral gully is the transition between a hillslope and a permanent drainage channel, it can be argued that both surface and subsurface flow may also converge at locations that become initiating points of the gullies.

Figure 2 Gullies showing different morphologies affected by soil hydrology with shallow and wide summer gully (left) and narrow and deep winter gully (right). Winter gully picture taken by I. Takken, Belgium.

Figure 3 Soil surfaces after erosion runs, except the soil box on the left was free drained and, on the right, set to seepage, showing the pore water effects on dominant erosion processes.

In the process-based Water Erosion Prediction Project (WEPP) model, the flow-driven rill detachment equation contains two soil dependent parameters, i.e., rill erodibility and critical shear stress:

$$D_c = K_r (\tau - \tau_c) \quad (1)$$

where Dc is the detachment capacity by rill flow of clear water (Kg s m), Kr is the rill erodibility (s m^{-1}), τ is the flow shear stress acting on the particle (Pa) and τc is the critical shear stress of the soil (Pa). τc expresses a critical value of flow stress that must be exceeded to start detaching soil from the shear flow. To be able to adjust soil erosion models for subsurface moisture condition, there is a need to define soil erosion parameters (rill erodibility and critical shear stress) as a function of the soil moisture condition.

The objectives of this research were to (1) use an empirical approach to measure the change in rill erodibility and critical shear stress in response to a change in subsurface hydraulic conditions; (2) propose a fluidized bed approach to calculate the soil's inherent critical shear stress; and (3) isolate the hydraulic gradient effects on the measured critical shear stress.

MATERIALS AND METHODS

Fluidized Bed Process A fluidized bed is obtained when a solid particle bed is forced to behave as a fluid by the introduction of a pressurized fluid in the pore space of the particle bed. For non-cohesive particles, the fluidization point is reached when the working forces of the fluid phase (buoyancy and velocity) overcome the weight of the solid particles and the pressure drop at fluidization is described by Ergun's equation (Yang, 2003):

$$\Delta P = \left(150 \frac{(1-\varepsilon)^2 * \mu * V_s}{\varepsilon^3 D_p^{\,2}} + 1.75 \frac{(1-\varepsilon) * \rho_f * V_s^{\,2}}{\varepsilon^3 D_p} \right) * L \quad (2)$$

where ΔP is the pressure drop (Pa), L is the thickness of the bed (m), Dp is the diameter of the

solid particles (m), ρ_f is the density of the fluid (kg m^{-3}), Vs is the superficial upward velocity of the fluid (m s^{-1} , note: Vs = Q/A, where Q is the flow rate, m^3 s^{-1} , and A is the cross sectional area of the bed), ε is the porosity of the bed, and μ is the dynamic viscosity of the fluid (Pa s).

For cohesive materials like soils, a cohesion term can be added to the Ergun's equation:

$$\frac{\Delta P}{L} = \left(150 \frac{(1-\varepsilon)^2 \cdot \mu \cdot V_{sf}}{\varepsilon^3 D_{psm}{}^2} + 1.75 \frac{(1-\varepsilon) \cdot \rho_f \cdot V_{sf}{}^2}{\varepsilon^3 D_{psm}} \right) = \left(\rho_p - \rho_f \right) \cdot g + \frac{C_o}{L} \tag{3}$$

where Co is the cohesion term (Pa). To account for the heterogeneity of the particle sizes in the soil bed, the Sauter mean diameter Dpsm is used. The Sauter mean diameter also known as the volume-surface mean defines the average particle size based on the specific surface area per unit volume or per unit weight. In our case, only the sand and silt fraction are considered, as the clay fraction itself is difficult to fluidize (Yang, 2003).

Liu (2007) found that wall friction is present in a fluidized bed of diameter less than 0.03m and that the amount of friction per bed volume is independent of the characteristics of the bed material. In this research, we had to use a small diameter bed (0.012 m) because trials with larger diameter beds resulted in preferential flows. For the same volume V of cohesive material such as soil, the difference between theoretical and observed pressure drop is the sum of the cohesion and the wall friction (*wf*):

$$\frac{\Delta p}{L}_{Ergun} - \frac{\Delta p}{L}_{Observed} = \frac{C_o}{L} + wf \tag{4}$$

Therefore using the same volume of cohesive and non-cohesive materials, we can determine the cohesion within the cohesive bed material.

Assuming that the critical shear stress is the resultant of 2 perpendicular forces (the cohesion forces component applied to the non exposed half of a particle and the weight of the particle), the critical shear stress can be approximated using the following equation.

$$\tau_{cr} = \sqrt{\left(\frac{\frac{C_o}{L} * D_{psm}}{2} \right)^2 + \left(\frac{\frac{4}{3} * \pi * \left(\frac{D_{psm}}{2} \right)^3 * \left(\rho_p - \rho_f \right) * g}{\frac{1}{2} * \pi * D_{psm}{}^2} \right)^2} \tag{5}$$

This value can be compared to measured values of critical shear stress under different hydraulic gradients to determine the impact of each treatment.

Flume Experiments The soil used in this study was collected in the southern part of Tippecanoe County, IN. The soil is a loess derived silt loam with 18% sand, 62% silt and 20% clay. Once collected, the soil was ground and sieved through a 2mm sieve before its use in the experiments.

A mini-flume measuring 0.5m long 0.045m wide and 0.13m deep was used for the soil erodibility and critical shear stress measurement. The flume had drain holes at the bottom that can be used to control upward seepage flow or allow downward drainage. The upward flow is controlled by a Marriott bottle equipped with a flow control valve. The downward movement of water through the soil is controlled by a drainage tube set at a desired water table level. Five different soil subsurface hydraulic head were studied, i.e., -0.10 m, -0.05 m, 0 m, 0.05 m, and 0.10 m, where negative values indicate drainage condition and positive values as seepage condition. The runs were made at 2% and 5% slopes with three levels of inflow: 0.57, 1.8 and 2.5 L min^{-1}.

Since the critical shear stress is often derived from the regression procedure as the intercept of a linear regression between flow shear stress and soil loss, this process may not reveal small differences in critical shear stress values. For this reason, we directly determined the shear stress associated with incipient detachment of particles by slowly increasing the flow until erosion started in the mini-flume.

Fluidized Bed Experiments For these tests, we used uniform size glass beads as the non-cohesive material with the size, i.e., $2.43*10^{-4}$ m, obtained from Stokes' law. An average particle size of $2.62*10^{-5}$ m was obtained for the test soil using the Sauter mean diameter which is the average particle size based on the specific area per unit volume (Yang, 2003).

The experiment was conducted for two material thicknesses, i.e., 0.10 m and 0.05 m, to check for any depth effect on the fluidization flow velocity. To identify the point of fluidization, the upward flow was slowly increased until sediments started exiting the tube and bubbling appeared in the tube. A theoretical velocity for bed fluidization was calculated for the soil assuming that the cohesion term is not present.

RESULTS AND DISCUSSION

Effect of vertical hydraulic gradient on rill erodibility Figure 4 is a plot of rill detachment against flow shear stress, with data pooled for seepage and drainage conditions. Originally, we made a plot with each hydraulic gradient treatment identified and we found a general trend of an increasing hydraulic gradient effect on rill detachment as the pore water pressure was increased from drainage to seepage. Nevertheless, the data scatter makes it difficult to compare the hydraulic gradient effects at 0.05 m increments. However, when we grouped the data for seepage and drainage conditions, it became clear that the shift in pore water pressure from drainage to seepage condition significantly affected the erodibility which is the slope of the rill detachment rate plotted against the flow shear stress. The detachment rate showed little variation between treatments in the low range of shear stress (< 1Pa). This indicates that using the intercept of a linear regression procedure to obtain the critical shear stress value may not be adequate to reveal the hydraulic gradient effects on the critical shear stress values.

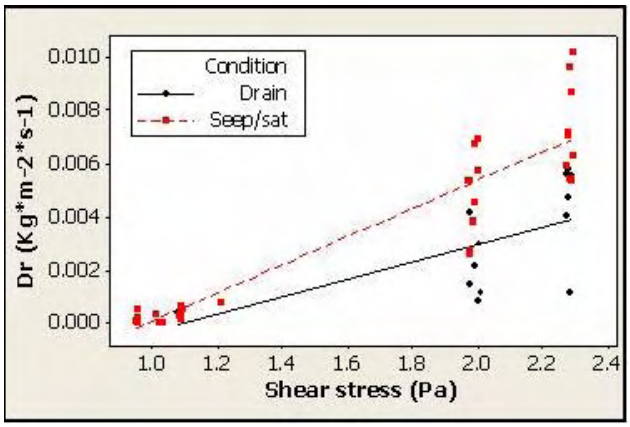

Figure 4 Rill detachment rate as a function of flow shear stress where data from different levels of hydraulic gradients were pooled together as drainage (Drain) when the pore water pressure was negative and as seepage/saturation (Seep/sat) for positive pore pressure.

Effect of vertical hydraulic gradient on critical shear stress Results from the visual observation of the incipient soil detachment and use it to calculate the critical shear were plotted in Figure 5. It shows a general decreasing trend in the critical shear stress when the pore water pressure was increased, but the trend appears to be more pronounced under the drainage condition as compared to that for the seepage condition. We believe these different hydraulic gradient effects can be explained.

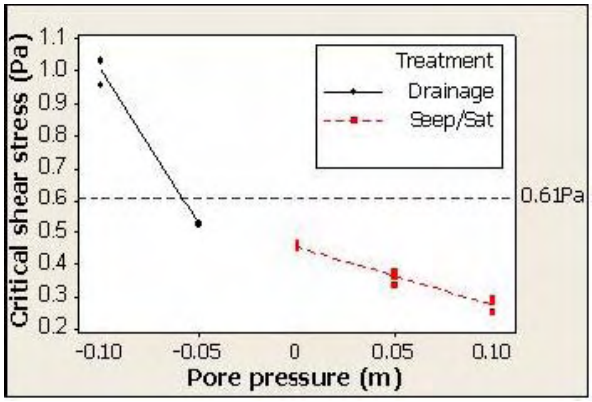

Figure 5 Relationships between critical shear stress and pore pressure showing different effects when the pore water pressure was changed from drainage to seepage.

The critical shear stress of the soil can be partitioned into 5 different components: a weight component, a buoyancy component, a matric suction component, a velocity component and the intrinsic cohesion component:

$$\tau_c = w + b + \varphi + \nu + C_o \tag{6}$$

where w is the weight component, b is the buoyancy component, φ is the matric suction component, ν is the vertical velocity component measured at the soil surface and Co is the intrinsic cohesion. We can then define the apparent cohesion term Ca as the sum of the pressure component, the velocity component and the intrinsic cohesion.

$$C_a = C_o + \varphi + \nu \tag{7}$$

A vertical downward flow of water (negative hydraulic gradient) results in a positive effect of the pressure component (matric suction) φ as well as a positive effect of the velocity component (infiltration) v. The apparent cohesion of a soil undergoing downward water flow would then be greater than that of a soil undergoing a positive hydraulic gradient as in the latter case, upward flow of water would cause a negative effect of the pressure component φ and a negative impact of the velocity component (upward seepage) *v*.

In the WEPP model, the hydraulic conductivity of the soil is negatively related to soil erosion. A high hydraulic conductivity implies a high infiltration, and consequently a low surface runoff and erosion. The results of this study suggest that this is true when the soil is in drainage condition. In seepage condition, a high hydraulic conductivity will lead to a high seepage velocity, reducing the cohesion of the soil. The hydraulic conductivity is then negatively related to soil erosion under the drainage condition and positively related to soil erosion under the seepage condition.

Another implication of our findings is that under drainage conditions, a shallow soil with an underlying highly conductive layer will reduce soil erosion compared to a deep soil in the same condition. Based on Darcy's law, the infiltration velocity will be higher in the shallow soil leading to an increase in the soil's apparent cohesion. But under seepage condition, the shallow soil will undergo increased erosion compared to the deeper soil, as the seepage velocity will be higher in the shallow soil.

Critical Shear Stress Measured From Fluidized Bed Technique The measured fluidization velocity was higher than the predicted fluidization velocity using Ergun's equation for both glass beads and soil beds. The ratio of measured over predicted fluidization velocity was on average 1.89 for the glass beads bed and 18.5 for the soil bed. The larger ratio indicates a significant contribution of cohesion to the measured velocity of fluidization for the soil. The thickness of both soil and glass beads beds did not show any impact on the measured fluidization velocity. This is expected for the glass beads bed, based on Ergun's equation (Eq. (2)); but for the soil bed, it implies that the cohesion per unit length Co/L was a constant in our experiment. Grinding and sieving the soil prior to the experiment contributed to maintaining a homogeneous cohesion throughout the entire soil bed.

We found the average difference between measured and predicted pressure drop was $8.284*10^3$ Pa/m for the glass beads bed and $1.312*10^5$ Pa/m for the soil bed, these values suggesting that the pressure drop associated with the cohesion is Co/L = $1.23*10^5$ Pa/m. The critical shear stress obtained from this cohesion value using Eq. (5) was 1.61 Pa.

The critical shear stress determined using the fluidized bed method was larger than all the measured critical shear stress values obtained from the other experiments. We expected the intrinsic critical shear stress to be close to the critical shear stress of the soil under a pressure head of 0m (around 0.5 Pa). The inevitable preferential flow present especially in the soil bed during fluidization is largely responsible for the slight overestimation.

With some improvements, the fluidized bed method appears promising for soil erosion applications. Beside the estimation of intrinsic critical shear stress as shown in this paper, the fluidized bed approach has the potential of predicting seepage induced soil erosion. By combining the topographic wetness index to the thickness and the hydraulic conductivity of the soil, one can predict the likelihood of seepage at a specific location. The seepage velocity can be predicted and introduced in the fluidized bed approach to determine the loss of cohesion due to seepage and hence adjust the critical shear stress.

CONCLUSION

In this research, we showed empirically the dependency of both soil erodibility and critical shear stress on the pore water pressure as we varied the near-surface hydraulic gradient. A difference in the critical shear stress values could not be found by the commonly used regression procedure. By visually determining the incipient detachment of soil particles, we showed that the critical shear stress is quasi linearly dependent on the soil vertical hydraulic gradient with the drainage condition affecting the critical shear stress differently from the seepage condition.

The fluidized bed approach that we propose for critical shear stress calculation seemed to closely approximate the true inherent critical shear stress of the soil. The concept of soil fluidization could also be used to improve seepage induced erosion models. The critical shear stress and the erodibility of a soil are parameters that need to be adjusted for the vertical hydraulic gradient in soil erosion models.

REFERENCES

Bryan, R., and Rockwell, D. (1998). Water table control on rill initiation and implications for erosional response. Geomorphology 23: 151-169.

Fox, G., Wilson, G., Periketi, R., and Cullum, R. (2006). Ssediment transport model for seepage erosion of streambank sediment. Journal of Hydrologic Engineering 6: 603-611.

Fox, G., Chu-agor, M., and Wilson, G. (2007). Erosion of noncohesive sediment by ground water seepage: lysimeter experiments and stability modeling. Soil Science Society of America Journal 71:1822-1830.

Huang, C., and Laflen, J. (1996). Seepage and soil erosion for a clay loam soil. Soil Science Society of America Journal 60: 408-416.

Liu, X., Xu G., Gao S. (2007). Micro fluidized beds: Wall effect and operability. Chemical Engineering Journal 137: 302–307.

Nachtergaele, J., Poesen, J., Vandekerckhove, L., Oostwoud Wijdenes, L., and Roxo, M. (2001). Testing the ephemeral gully erosion model (EGEM) for two Mediterranean environments. Earth Surf. Processes Landforms, 26: 17–30.

Owoputi, L., and Stolte, W. (2001). The role of seepage in erodibility. Hydrological Processes 15: 13–22.

Römkens, M., Helming, K., and Prasad, S. (2001). Soil erosion under different rainfall intensities, surface roughness, and soil water regimes. Catena 46: 103–123.

Simon, A., and Collison, A. (2001). Pore-water pressure effects on the detachment of cohesive streambeds: Seepage forces and matric suction. Earth Surface Processes and Landforms 26: 1421-1442.

Yang W. (2003). Handbook of Fluidization and Fluid-Particle systems. Siemens Westinghouse Power Corporation, Pittsburgh, Pennsylvania.

Zheng, F., Huang, C., and Norton, L.D. (2000). Vertical Hydraulic Gradient and Run-On Water and Sediment Effects on Erosion Processes and Sediment Regimes. Soil Science Society of America Journal 64: 4-11.